



ELSEVIER

Biophysical Chemistry 116 (2005) 175 – 185

---



---

 Biophysical  
Chemistry
 

---



---

<http://www.elsevier.com/locate/biophyschem>

## Bioluminescence regenerative cycle (BRC) system: Theoretical considerations for nucleic acid quantification assays

Arjang Hassibi<sup>b,c</sup>, Christopher Contag<sup>d</sup>, Marcel O. Vlad<sup>e</sup>, Maryam Hafezi<sup>d</sup>, Thomas H. Lee<sup>b</sup>,  
Ronald W. Davis<sup>a</sup>, Nader Pourmand<sup>a,\*</sup>

<sup>a</sup>Stanford Genome Technology Center, Stanford University, 855 California Avenue, Palo Alto, CA 94304, USA

<sup>b</sup>Center for Integrated Systems, Stanford University, Stanford, CA, USA

<sup>c</sup>Xagros Technologies Inc., Mountain View, CA, USA

<sup>d</sup>Department of Pediatrics, Stanford University, Stanford, CA, USA

<sup>e</sup>Department of Chemistry, Stanford University, Stanford, CA, USA

Received 2 November 2004; received in revised form 13 April 2005; accepted 13 April 2005

### Abstract

A novel application of bioluminescence for nucleic acid quantification, the bioluminescence regenerative cycle (BRC), is described in theoretical terms and supported by preliminary experimental data. In the BRC system, pyrophosphate (PPi) molecules are released during biopolymerization and are counted and correlated to DNA copy number. The enzymes ATP-sulfurylase and firefly luciferase are employed to generate photons quantitatively from PPi. Enzymatic unity-gain positive feedback is implemented to amplify photon generation and to compensate for decay in light intensity by self-regulation. The cumulative total of photons can be orders of magnitude higher than in typical chemiluminescent processes. A system level theoretical model is developed, taking into account the kinetics of the regenerative cycle, contamination, and detector noise. Data and simulations show that the photon generation process achieves steady state for the time range of experimental measurements. Based on chain reaction theory, computations show that BRC is very sensitive to variations in the efficiencies of the chemical reactions involved and less sensitive to variations in the quantum yield of the process. We show that BRC can detect attomolar quantities of DNA ( $10^{-18}$  mol), and that the useful dynamic range is five orders of magnitude. Sensitivity is not constrained by detector performance but rather by background bioluminescence caused by contamination by either PPi or ATP (adenosine triphosphate).

© 2005 Published by Elsevier B.V.

*Keywords:* Chemiluminescence; Bioluminescence; Gene expression; Nucleic acid; Polymerization; Enzyme kinetics; Positive feedback

### 1. Introduction

A significant technical challenge in the field of genomics is to find more flexible methods for quantifying nucleic acids. A label-independent and more sensitive method for parallel detection and quantification of nucleic acid would significantly add to our arsenal of tools for analyzing genomes. Presently, real-time quantitative polymerase chain reaction (Q-PCR), a label-based assay that implements PCR thermo-cycling platforms [1–4], is commonly used. In one

application of the method, a probe is designed to consist of an oligonucleotide with a reporter and a quencher dye. The oligonucleotide anneals specifically to a target of interest between the forward and reverse primer binding sites. The exonuclease activity of the polymerase cleaves the probe, resulting in an increase in the fluorescence intensity of the reporter dye, a process that occurs in every cycle and does not interfere with the accumulation of PCR product. This approach is applicable to small numbers of target DNA molecules within a sample.

In contrast, nucleic acid microarrays [5–7] provide a systematic and parallel platform for multiparametric exploration of the genome. Microarray technology, in principle and practice, is an extension of hybridization-based methods

\* Corresponding author. Tel.: +1 650 812 2002; fax: +1 650 812 1975.

E-mail address: [pourmand@stanford.edu](mailto:pourmand@stanford.edu) (N. Pourmand).

that have been used to identify and quantify nucleic acids in biological samples [8,9]. The basic concept here comes from the specificity and affinity of complementary base-pairing for handling specific DNA or RNA target molecules, with fluorescent labeling to detect their quantity. A chemiluminescence assay employing the enzyme hypoxanthine phosphoribosyltransferase and the substrates hypoxanthine and luminol to determine inorganic pyrophosphate has been described previously [10]. The sensitivity of the previously described assay, however, is in the picomole region.

In this study we explore theoretical considerations underlying the BRC system and use this as a basis to explore the development of a method that does not require any molecular modification or labeling and merely counts the inorganic pyrophosphate (PPi) molecules released during the polymerization of the nucleic acid by a polymerase enzyme (e.g., Klenow [11]). This technique implements a bioluminescence regenerative cycle, activated by the generated PPi molecules which, in quantity, are proportional to the number of target molecules. The regenerative cycle uses ATP-sulfurylase enzyme [12,13] to convert PPi to ATP (adenosine triphosphate), which it does by consuming APS (adenosine phosphosulfate) and firefly luciferase [14,15]. In the presence of luciferin the system consumes ATP as an energy source to generate photons as a detectable signal, and again yields PPi as a by-product (Fig. 1). We have shown that the photon emission rate with PPi regeneration achieves steady state conditions and that it is also a monotonic function of the introduced PPi. For very low concentrations of PPi (lower than  $10^{-8}$  M), the total number of photons generated in a fixed time interval is proportional to the number of PPi molecules, and thus proportional to the number of nucleic acid molecules present in the solution.

The basic concept of enzymatic light generation from PPi molecules was introduced in 1985 and reported on subsequently in 1987 and 1992 [16–18]. Other applications of this enzymatic detection method, including single nucleotide polymorphism (SNP) detection [19] and DNA sequencing by synthesis [20,21], have also been studied.

Here, we first present theoretical concepts supporting our exploration of sensitive, label-free methods for quantifying nucleic acid, and follow with experimental data that have helped to identify the additional steps necessary to accurately quantify extremely small numbers of nucleic acid copies in low-density assays. Significantly, the BRC system reduces the need for high levels of ATP or PPi, and lowers background noise from APS such that it is possible to quantify low concentrations of nucleic acids even in the presence of contaminants and other potential sources of noise. As indicated in our experimental section, the new system described here has an intrinsic controllable assay dynamic range of about five orders of magnitude, and is sensitive to  $10^5$  copies of target nucleic acid.

## 2. Theoretical concepts

### 2.1. Pyrophosphate generation

In polymerase-catalyzed reactions, PPi molecules are generated when nucleotides (dNTPs) are incorporated into the nucleic acid chain. For each addition of a nucleotide, one PPi molecule is cleaved from the dNTP by the polymerase enzyme (e.g., Klenow [11,22]) and released into the reaction buffer. For DNA molecules we have



where  $n$  is the position of the 3' end of the primer in the DNA strand. If one assumes that the strand is completely polymerized, then the number of PPi molecules  $N_{\text{PPi}}$  released during this process can be expressed as

$$N_{\text{PPi}} = N_{\text{NA}}(L_{\text{NA}}L_{\text{P}}) \quad (2)$$

where  $N_{\text{NA}}$  is the total number of primed nucleic acid molecules present in the reaction buffer, and  $L_{\text{NA}}$  and  $L_{\text{P}}$  are the lengths of the nucleic acid chain and the primer, respectively.

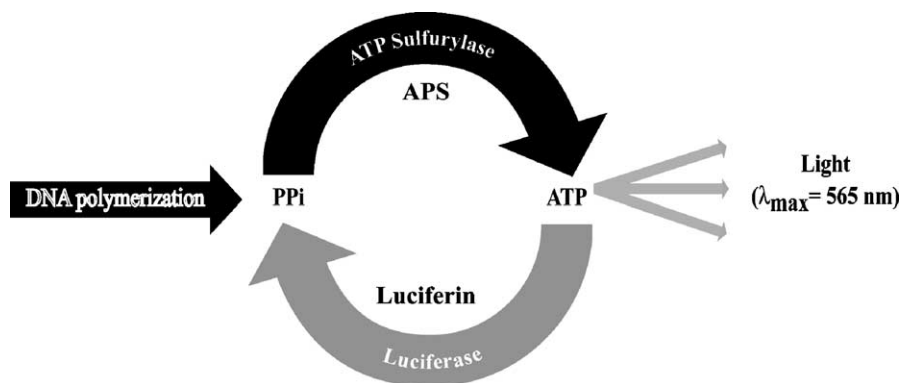


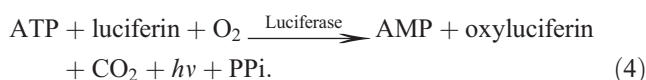
Fig. 1. Bioluminescence regenerative cycle (BRC) with ATP-sulfurylase and firefly luciferase process detecting the generated PPi molecules. The regenerative cycle uses the ATP-sulfurylase enzyme that converts PPi to ATP by consuming APS and firefly luciferase, which, in the presence of luciferin, consumes ATP as an energy source to generate photons as a detectable signal, again yielding PPi as a by-product.

## 2.2. Enzymatic bioluminescence cycle

To generate photons efficiently from the pyrophosphate release process, ATP-sulfurylase enzyme [12,13] is initially introduced to the system to catalyze the transfer of the adenylyl group from ATP to inorganic sulfate-producing adenosine 5'-phosphosulfate APS. This sulfurylase enzyme is ubiquitous in nature, although its physical role depends on the metabolic lifestyle of the organism. In the BRC assay we used the enzyme to generate ATP from pyrophosphate, by consuming APS:



To complete the chemical process we used firefly luciferase which, with a nominal turnover rate of 0.015/s [14,23], consumes the generated ATP to emit photons ( $\lambda_{\text{max}} = 565 \text{ nm}$ , Q.E.  $\approx 0.88$ ). This process consumes luciferin as a substrate and generates oxyluciferin, adenosine monophosphate (AMP),  $\text{CO}_2$  and PPi as by-products.



It is evident from Eqs. (3) and (4) that the PPi molecules generated at the end of the photon emission process by luciferase can again trigger the ATP synthesis reaction by ATP-sulfurylase, which results in a substrate cycling phenomenon (enzymatic positive feedback). Since the inherent characteristic of this positive feedback can regulate the total amount of ATP or PPi molecules in the solution, the light emission can be subsequently regulated without any decay. Because the chemical yield of PPi generation per ATP from luciferase is close to unity (always less than unity), we are able to model this phenomenon as an ideal unity-gain positive feedback (Fig. 2), which adjusts the process for the inhibition of light intensity degradation due to substrate consumption.

It is important to recognize that the number of photons generated by the regenerative cycle can potentially be orders of magnitude higher than the initial number of PPi (or ATP) molecules introduced to the system. Coupled with longer integration times, this results in greatly increased sensitivity.

In Fig. 3 the simulation results and actual experimental results of a BRC system compared to an ATP assay (no enzymatic feedback) is shown. As is evident, substrate

cycling stabilizes the light intensity near its temporal peak. In contrast, no such stabilization occurs in the assay that lacks enzymatic feedback.

## 2.3. Photon generation rate

Given that polymerase affects neither the luminescence process nor the enzymatic feedback, the kinetics of ATP-sulfurylase and luciferase [23] determine the steady state photon generation rate of BRC. As shown in Fig. 2 the system consists of two different enzymatic processes with a unity-gain positive feedback. At saturating concentrations of APS and luciferin, we can assume that the cycle has reached a steady state in which there is no change in the concentration of cycling substrates.

$$\frac{dN_{\text{ATP}}(t)}{dt} = \frac{dN_{\text{PPi}}(t)}{dt} = \text{cte}. \quad (5)$$

Eq. (5) states that the overall rates of PPi generation (luciferase) and consumption (ATP-sulfurylase) are equal; consequently, if the turnover rate of luciferase and ATP-sulfurylase are  $k_L$  and  $k_a$ , respectively, then

$$k_L \left( \frac{N_{\text{ATP}}(t)}{V} \right) = k_a \left( \frac{N_{\text{PPi}}(t)}{V} \right). \quad (6)$$

The steady state assumptions for Eqs. (5) and (6) are valid for the time range of experimental measurements (1–10 s) and even for larger time intervals of up to 1 min. As is shown below in the experimental results, a slow exponential decay with a time constant of about 10 min eventually emerges. This exponential decay leads to the violation of the steady state conditions but, because it occurs out of the range of measurements, does not undermine our approach. The values of  $k_L$  and  $k_a$  depend on the concentration of the enzymes, the characteristics of the reaction buffer and the availability of substrates (APS for ATP-sulfurylase, and luciferin for luciferase); however, in typical BRC assays, the actual values of these parameters change very little during the light generation process. In addition, the turnover rate of ATP-sulfurylase in the BRC assay is adjusted so that it generally stays much higher than that of luciferase ( $k_L \ll k_a$ ); hence

$$\frac{N_{\text{PPi}}(t)}{N_{\text{ATP}}(t)} = \frac{k_L}{k_a} \approx 0, \quad (7)$$

which states that the relative number of PPi molecules in the reaction buffer compared to the number of ATP molecules at any given time is almost zero during steady state. Further-

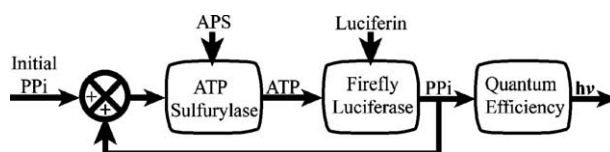


Fig. 2. Bioluminescence regenerative cycle diagram. The cycles consists of ATP-sulfurylase which converts PPi to ATP with yield of one, followed by luciferase which converts the generated ATP to PPi, and emits a single photon (quantum efficiency of 0.8). After the bioluminescence step the PPi by-product is recycled again by ATP-sulfurylase, resulting in a regulated enzymatic cascade.

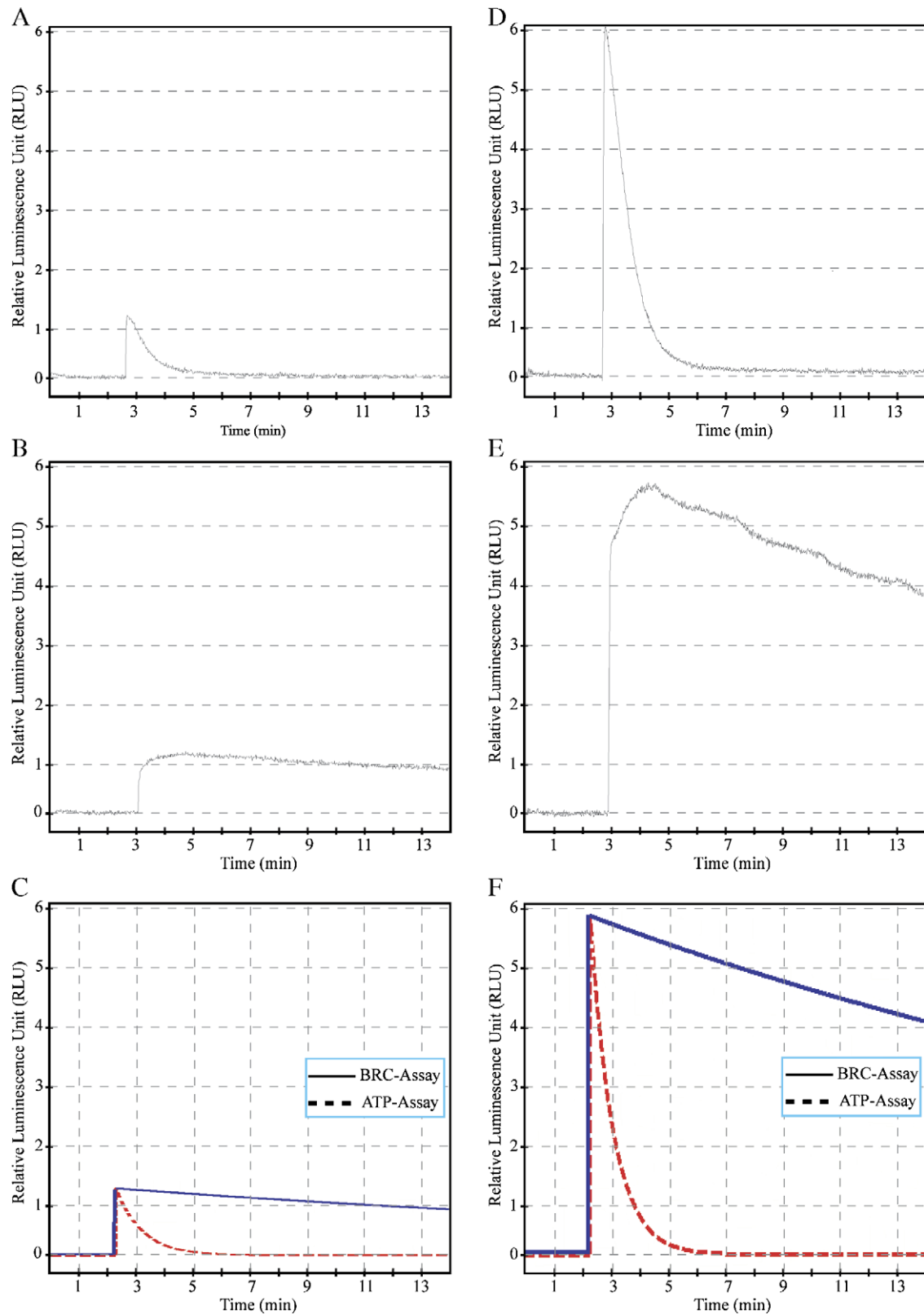


Fig. 3. Comparison of real data and simulated results based on enzyme kinetics measurements [12,23] showing the relative light intensity in the ATP assay and the BRC system (0.1 mM luciferin, 10  $\mu$ M APS). The ATP assay is shown at (A) 1 pmol ATP and (D) 5 pmol ATP. The BRC assay is shown at (B) 1 pmol ATP and (E) 5 pmol ATP. The simulated results for both assays are shown together at (C) 1 pmol ATP and (F) 5 pmol ATP.

more, if we suppose that the initial number of PPi molecules from the polymerization of the target nucleic acid is  $(N_{\text{PPi}})_0$ , then the total number of ATP plus PPi at any given time in the process will be equal to  $(N_{\text{PPi}})_0$ . Considering Eq. (7) we can conclude that the total number of ATP molecules in the BRC at steady state is then equal to the total initial number of PPi molecules,  $(N_{\text{PPi}})_0$ , introduced to the system:

$$N_{\text{ATP}}(t) = (N_{\text{PPi}})_0. \quad (8)$$

Eq. (8) indicates that the photon-generation process is a function of the turnover rate of luciferase only rather than of ATP-sulfurylase. The simplified equation expressing light intensity from unit of volume  $I(t)$  is

$$I(t) = \alpha \cdot \frac{d}{dt} \left( \frac{N_{\text{ATP}}}{V} \right) = \left( \frac{\alpha \cdot k_L}{V} \right) \cdot N_{\text{ATP}}(t), \quad (9)$$

or

$$I(t) = \left( \frac{\alpha \cdot k_L}{V} \right) \cdot (N_{\text{PPi}})_0 \quad (10)$$

where  $V$  is the volume of the reaction buffer, and  $\alpha$  is the quantum efficiency of the bioluminescence process. Combining Eq. (10) with the number of nucleic acid molecules in the solution (2), we have:

$$I(t) = \left( \frac{\alpha \cdot k_L}{V} \right) \cdot N_{\text{NA}} \cdot (L_{\text{NA}} - L_{\text{P}}). \quad (11)$$

Eq. (11) shows the linear proportionality of generated light intensity  $I(t)$  to the initial number of nucleic acid molecules within the assumed region. If we accumulate photons for a time interval  $T$  (integration time) from the whole reaction volume, then the total number of emitted photons  $N_{\text{ph}}$  is

$$N_{\text{ph}} = (\alpha \cdot k_L) \cdot T \cdot N_{\text{NA}} (L_{\text{NA}} - L_{\text{P}}). \quad (12)$$

Thus the total number of photons received by the detector (e.g., CCD camera) depends on the integration time and the number of molecules present in the solution. By controlling the integration time we are able to change the gain of the system and potentially increase the sensitivity. In typical bioluminescence assays where there is no enzymatic feedback, we introduce  $N = N_{\text{NA}}$  substrate molecules which, over time, will be converted to  $\alpha' N_{\text{NA}}$  photons, where  $\alpha'$  is the chemiluminescence quantum efficiency. If we introduce the same number of molecules to a BRC process and compare the total photons generated in time interval  $T$ , then the signal amplification of the BRC system  $A_{\text{E}}$ , compared to the bioluminescence method is

$$A_{\text{E}} = \frac{(\alpha \cdot k_L) \cdot T \cdot N_{\text{NA}} \cdot (L_{\text{NA}} - L_{\text{P}})}{\alpha' \cdot N} = \left( \frac{\alpha}{\alpha'} \right) \cdot k_L \cdot T (L_{\text{NA}} - L_{\text{P}}). \quad (13)$$

#### 2.4. Detection error and background light

Two different phenomena ultimately limit the performance and sensitivity of the BRC system. One is the possibility of PPi and ATP background contamination by chemicals used in the buffer solution, and the other is the inherent noise of the detector (e.g., thermal and shot noise in a photodiode system). To model the presence of ATP, PPi or any other light-generating chemicals during the enzymatic cycle, we refer to them as an equivalent number of PPi molecules,  $C_{\text{PPi}}$ . Therefore Eq. (11) can be rewritten as:

$$I = (\alpha \cdot k_L) \cdot [N_{\text{NA}} \cdot L_{\text{NA}} - L_{\text{P}} + C_{\text{PPi}}]. \quad (14)$$

Although  $C_{\text{PPi}}$  is relatively low for common bioluminescence assays (on the order of 1 to 10 pM concentration), it can be an order of magnitude higher than the target nucleic acid concentration for gene expression applications. It is also likely for the value of  $C_{\text{PPi}}$  to vary between experiments by as much as 2.5-fold. To eliminate the effects of any possible background on the final measurement, we also measure the light intensity of the system in the absence of any excess PPi generated from polymerization. This control measurement serves as a reference point for quantification of the catalytically produced PPi. If the light intensity in the reference condition is  $I_r$ , then, by combining Eqs. (10) and (14), the value of  $N_{\text{NA}}$  can be derived from

$$N_{\text{NA}} = \left( \frac{1}{\alpha \cdot k_L} \right) \cdot \frac{I - I_r}{L_{\text{NA}} - L_{\text{P}}}, \quad (15)$$

and in terms of number of photons detected

$$N_{\text{NA}} = \left( \frac{1}{\alpha \cdot k_L} \right) \cdot \frac{N_{\text{ph}} - N_{\text{phr}}}{T \cdot (L_{\text{NA}} - L_{\text{P}})}. \quad (16)$$

To take into account the noise of the system, we assume that the total noise of the detector in the measurement  $n(t)$  is random and has a normal distribution  $N(0, \sigma)$  (mean of zero, and standard deviation of  $\sigma$ ). Thus, the apparent light intensity in the presence of detector noise  $I_{\text{V}}(T)$ , from the volume, is given by

$$I_{\text{V}}(t) = (\alpha \cdot k_L) \cdot N_{\text{NA}} \cdot (L_{\text{NA}} - L_{\text{P}}) + n(t). \quad (17)$$

Integrating Eq. (17) over a time interval  $T$ ,

$$N_{\text{ph}} \int_T I_{\text{V}}(\tau) d\tau = (\alpha \cdot k_L) \cdot N_{\text{NA}} \cdot (L_{\text{NA}} - L_{\text{P}}) T + \int_T n(\tau) d\tau. \quad (18)$$

As we can see in Eq. (18) the number of photons generated in a time interval  $T$  consists of a deterministic value plus the measurement noise integrated over time interval  $T$ . The new noise term has a normal distribution

with mean and standard deviation of zero and  $\sigma/\sqrt{T}$ , respectively; subsequently the maximum signal-to-noise power, considering no path loss, becomes:

$$\left(\frac{S}{N}\right) = \left(\frac{\alpha \cdot k_L N_{NA} \cdot (L_{NA} - L_P)}{\sigma^2}\right) \cdot T. \quad (19)$$

To calculate the error distribution of the measurement, initially we express the calculated number of nucleic acids,  $N'_{NA}$ , as

$$\begin{aligned} N'_{NA} &= \left(\frac{1}{\alpha \cdot k_L}\right) \cdot \frac{\int_T I_V(\tau) d\tau}{(L_{NA} - L_P) \cdot T} \\ &= \left(\frac{1}{\alpha \cdot k_L}\right) \cdot \frac{N_{ph} - N_{phr} + \int_T [n_1(\tau) - n_2(\tau)] d\tau}{(L_{NA} - L_P) \cdot T}, \end{aligned} \quad (20)$$

where  $n_1(t)$  and  $n_2(t)$  represent the noise induced by the detector in the actual and reference experiments, respectively. If we assume that  $n_1(t)$  and  $n_2(t)$  are not correlated but have the same normal statistical distribution, Eq. (17) can be rewritten as

$$N'_{NA} = N_{NA} + n'(t). \quad (21)$$

Hence  $n'(t)$ , the error distribution (statistical variation between the estimated value and the actual value) is finally defined by a normal distribution:

$$N'_{NA} - N_{NA} = n'(t) \rightarrow N\left(0, \sqrt{\frac{2}{T}} \cdot \frac{\sigma}{\alpha \cdot k_L (L_{NA} - L_P)}\right). \quad (22)$$

Eq. (22) states that in a typical BRC experiment, which comprises a reference (background) measurement and  $T$  second integration time, the estimated value always has an error with the mean of zero, and standard deviation proportional to the inverse square root of the integration time.

### 2.5. The BRC process as a chain reaction

The bioluminescence regenerative cycle is essentially a linear chain reaction involving two successive propagation steps, as shown in Eqs. (3) and (4). Starting from an initial PPI molecule generated by reaction (1), repetition of the successive processes (3) and (4) leads to the generation of large numbers of PPI molecules and their accumulation in the system, resulting in the amplification of the optical signal used in the detection process. Examining the BRC process from the point of view of the theory of chain reactions [24] leads to a better understanding of the chemistry of the process and makes

it possible to examine the efficiency of the detection from a point of view different from the one examined in the previous sections.

Two main variables in the theory of chain reactions are the chain length  $q$  and the reaction time  $\tau$ . The chain length  $q$  is the number of molecules of active intermediates (in our case PPI) generated, starting from a single reaction intermediate molecule followed by the repeated occurrence of the propagation steps until the process terminates. The reaction time  $\tau$  is the time interval that elapses from the start of the reaction by this single intermediate until the termination of the succession of propagation events. Even if the kinetics of the process is assumed to be deterministic, these two quantities are random variables obeying certain probability laws. We denote by  $\Phi(q, \tau)$  the probability density of these two random variables. By definition, this probability density obeys the normalization condition  $\int \Phi(q, \tau) d\tau = 1$ . To each of the propagation reactions (3) and (4), we introduce a label,  $\varepsilon = \pm$ , where the + sign means that the reaction takes place and the - sign means that the reaction does not take place (i.e., has terminated). We also introduce a reaction time  $\theta$  for each of the individual processes (3) and (4), and the joint probability densities for these two variables  $\psi_u(\varepsilon, \theta)$  where  $u=3, 4$  is the reaction label. The joint probability densities  $\psi_u(\varepsilon, \theta)$  obey the normalization conditions  $\sum_{\varepsilon=\pm} \int \psi_u(\varepsilon, \theta) d\theta = 1$ ,  $u=3, 4$ . We note that  $p_u(+)=\int \psi_u(+, \theta) d\theta$ ,  $u=3, 4$  is the probability that the reaction  $u$  takes place (the chemical efficiency of the reaction), whereas the complementary probability  $p_u(-)=\int \psi_u(-, \theta) d\theta=1-p_u(+)$ ,  $u=3, 4$  is the probability that the reaction does not take place and the process terminates. The probability densities  $\psi_u(\varepsilon, \theta)$  can be evaluated from the kinetics of the process by using the transit time theory [25].

The joint probability density  $\Phi(q, \tau)$  of the chain length and the reaction time can be evaluated from the individual probability densities  $\psi_u(\varepsilon, \theta)$  attached to the individual propagation reactions (3) and (4). By taking into account the different types of events that lead to  $q$  generating processes of the reaction intermediate followed by a termination process we come to:

$$\begin{aligned} \Phi(q, \tau) &= \underbrace{\{[\psi_3(+, \tau) \otimes \psi_4(+, \tau)] \otimes \dots \otimes [\psi_3(+, \tau) \otimes \psi_4(+, \tau)]\}}_{q \text{ times}} \\ &\quad \times \otimes [\psi_3(-, \tau) + \psi_3(+, \tau) \otimes \psi_4(-, \tau)] \end{aligned} \quad (23)$$

where  $\otimes$  denotes the convolution product. By integrating Eq. (23) over all possible values of the reaction time we obtain the probability  $\varphi(q)$  that the chain length is  $q$ . After lengthy manipulations we come to:

$$\varphi(q) = \int_0^\infty \Phi(q, \tau) d\tau = (P_{34}(+))^q [1 - P_{34}(+)], \quad (24)$$

where

$$P_{34}(+) = p_3(+)p_4(+), \quad (25)$$

is the total probability of propagation of the process, that is, the probability that an initial PPI generates an ATP molecule through the process (3) followed by the regeneration of PPI through the reaction (4). The average value and the dispersion of the chain length can be easily evaluated from Eq. (25), resulting in:

$$\langle q \rangle = \sum q \varphi(q) = P_{34}(+)/[1 - P_{34}(+)], \quad (26)$$

$$\langle \Delta q^2 \rangle = \sum (q - \langle q \rangle)^2 \varphi(q) = P_{34}(+)/[1 - P_{34}(+)]^2. \quad (27)$$

The evaluation of the statistical properties of the reaction time is more complicated. The generating function of the joint probability density  $\Phi(q, \tau)$  can be defined as  $\Xi(z, s) = \sum \int \Phi(q, \tau) z^q \exp(-s\tau) d\tau$ , where  $z$  and  $s$  are the  $Z$  and Laplace variables conjugated to the chain length and to the reaction time, respectively. The generating function  $\Xi(z, s)$  can be easily evaluated from Eq. (23). By evaluating the derivatives of  $\Xi(z, s)$  we can compute the various moments of the reaction time. In particular, we obtain the following expressions for the moments of first and second orders:

$$\langle \tau \rangle = \Sigma \int \tau \Phi(q, \tau) d\tau = \langle \theta_{34} \rangle / [1 - P_{34}(+)], \quad (28)$$

$$\begin{aligned} \langle \Delta \tau^2 \rangle &= \Sigma \int (\tau - \langle \tau \rangle)^2 \Phi(q, \tau) d\tau \\ &= \frac{\langle (\Delta \theta_{34})^2 \rangle}{1 - P_{34}(+)} + \frac{\langle \theta_{34} \rangle^2 P_{34}(+)}{[1 - P_{34}(+)]^2}, \end{aligned} \quad (29)$$

$$\begin{aligned} \langle \Delta \tau \Delta q \rangle &= \Sigma \int (\tau - \langle \tau \rangle)(q - \langle q \rangle) \Phi(q, \tau) d\tau \\ &= \frac{\langle \theta_{34} \rangle^2 P_{34}(+)}{[1 - P_{34}(+)]^2}, \end{aligned} \quad (30)$$

where  $\theta_{34}$  is the reaction time attached to a single succession of reactions (3) and (4). From Eqs. (28), (29) and (30) we can evaluate the normalized correlation function of the chain length  $q$  and the reaction time  $\tau$ . We have:

$$\begin{aligned} \rho(q, \tau) &= \frac{\langle \Delta q \Delta \tau \rangle}{\sqrt{\langle \Delta q^2 \rangle \langle \Delta \tau^2 \rangle}} \\ &= \left\{ \left[ \frac{1 - P_{34}(+)}{P_{34}(+)} \right] \left[ \frac{\langle (\Delta \theta_{34})^2 \rangle}{\langle \theta_{34} \rangle^2} \right] + 1 \right\}^{-\frac{1}{2}}. \end{aligned} \quad (31)$$

## 2.6. Physico-chemical significance of foregoing theoretical results

From Eq. (26) it follows that the BRC process leads to a significant amplification of the response signal only if the average reaction chain length  $\langle q \rangle$  is very large. According to Eqs. (25) and (26) it is possible for  $\langle q \rangle$  to be very large only if both chemical efficiencies  $p_3(+)$  and  $p_4(+)$  of reactions (3) and (4) are very close to unity. We must draw attention to the fact that the chemical  $p_4(+)$  efficiency of reaction (4) is different from the quantum efficiency  $\alpha'$ . The chemical efficiency  $p_4(+)$  is the average fraction of the ATP molecules that regenerate the PPI molecules, whereas the quantum efficiency  $\alpha'$  is the average number of photons released in the process. The average number of photons  $\langle \Gamma \rangle$  and the corresponding dispersion  $\langle \Delta \Gamma^2 \rangle$  produced by the total offspring of an initial PPI molecule can be easily evaluated. We have

$$\langle \Gamma \rangle = \Sigma \alpha' q \varphi(q) = \alpha' \langle q \rangle, \quad (32)$$

$$\langle \Delta \Gamma^2 \rangle = \Sigma (\alpha' q - \langle \Gamma \rangle)^2 \varphi(q) = \alpha'^2 \langle \Delta q^2 \rangle. \quad (33)$$

From Eqs. (32) and (33) we note that the efficiency of the BRC cycle, measured by  $\langle \Gamma \rangle$  which plays the role of an average amplification factor, is affected by the chemical and quantum efficiencies of the regeneration process (4) in different ways. The average amplification factor  $\langle \Gamma \rangle$  varies hyperbolically with the chemical efficiency  $p_4(+)$  and is very sensitive to its variation, especially in the region where  $p_4(+)$  is close to unity. On the other hand, the dependence of the amplification factor  $\langle \Gamma \rangle$  on the quantum efficiency  $\alpha'$  is linear and thus the resulting signal is reasonably large provided that  $\alpha'$  is of the order of magnitude of unity, a condition that is fulfilled by the experiments reported below, for which  $\alpha' \sim 0.88$ .

For large numbers of regeneration events, the chemistry of the process induces fluctuations of the total number  $\Gamma$  of photons produced by the offspring of an initial PPI molecule. The contribution of the chain reaction to the fluctuation of the number of photons can be evaluated by computing the relative fluctuation  $\chi(\Gamma)$  of  $\Gamma$ :

$$\chi(\Gamma) = \langle \Gamma \rangle / \sqrt{\langle \Delta \Gamma^2 \rangle} = \sqrt{p_3(+)p_4(+)}. \quad (34)$$

Surprisingly, the relative fluctuation  $\chi(\Gamma)$  is independent of the quantum efficiency  $\alpha'$  of the reaction (4) and depends only on the chemical efficiencies of the reactions (3) and (4). We note that for large chemical efficiencies,  $p_3(+)$ ,  $p_4(+)$   $\sim 1$ , we have  $\chi(\Gamma) \sim 1$  and thus the average value and the dispersion of the average number of photons are approximately equal  $\langle \Gamma \rangle \sim \langle \Delta \Gamma^2 \rangle$ , which suggests that  $\Gamma$  obeys Poissonian statistics. Since a Poissonian distribution can be represented with fairly accurately by a Gaussian (normal) distribution, this result is consistent with the earlier assumption that detection errors can be represented by a

normal distribution. Of course, chemical fluctuations are only one component of detection errors.

We can also examine the steady state assumption from the point of view of chain reaction theory. We start out by noting that, according to Eqs. (26) and (28), we have:

$$\langle \tau \rangle = \langle q \rangle \langle \theta_{34} \rangle / P_{34}(+) \sim \langle q \rangle \langle \theta_{34} \rangle \text{ as } p_3(+), p_4(+)\sim 1. \quad (35)$$

That is, the reaction time is proportional to the average chain length. If the BRC process is very efficient,  $p_3(+)$ ,  $p_4(+)\sim 1$ , we have  $\langle q \rangle \gg 0$  and thus,  $\langle \tau \rangle \gg \langle \theta_{34} \rangle$ , which justifies the use of the steady state assumption.

### 3. Experimental section

We undertook preliminary experiments to probe the assumptions outlined in the foregoing theoretical section. These studies were designed primarily to demonstrate that an enzymatic regenerative cycle for the luciferase reaction was possible. In reducing the BRC method to practice, a number of considerations emerged that allowed us to assess the performance characteristics of an assay based on the BRC system.

#### 3.1. Materials and methods

##### 3.1.1. Synthesis and purification of oligonucleotides

The oligonucleotides B-MBPup, (5'-Biotin CGGCGAT-AAAGGCTATAACGG), MBPup (CGGCGATAAAGGCTATAACGG), B-MBPR1 (5'-Biotin CTGGAACGCTTTGTCCGGGG), MBPR1 (5'-CTGGAACGCTTTGTCCGGGG) and oligo-loop, (5'TTTTTTTTTTTTTTTTTTTTGC-TGGAATTCGTCAGACTGGCCGTCGTTTTACAACG-GAACGTTGAAAACGACGGC), were all synthesized and HPLC purified by MWG Biotech (High Points, NC, USA).

##### 3.1.2. Template preparation

The biotinylated PCR products were immobilized onto streptavidin-coated superparamagnetic beads, Dynabeads™ M280-Streptavidin (DynaL A.S., Oslo, Norway). Single-stranded DNA (ssDNA) was obtained by removing the supernatant after incubation of the immobilized PCR product in 100 mM NaOH for 3 min. Extension primers MBP-up or MBP-R1 (5 pmol) were hybridized to the immobilized ssDNA strand that was obtained from an amplified product via polymerase chain reaction (PCR).

##### 3.1.3. BRC assay

The immobilized single-stranded PCR product was resuspended in annealing buffer (10 mM Tris-acetate pH 7.75, 2 mM Mg-acetate), and primers were added to the single-stranded templates. Hybridization of the template and primers was performed by incubation at 95 °C for 3 min, 55 °C for 5 min and then cooling to room temper-

ature. Primer extension was initiated by the addition of exonuclease-deficient Klenow DNA polymerase (10 U; Fermentas, NY, USA) and all four nucleotides (dCTP, dGTP, dTTP and dATP $\alpha$ S) at 10  $\mu$ M final concentration in the extension mixture. During pyrosequencing, the nucleotide analog dATP $\alpha$ S is substituted for dATP to minimize background signal from the interaction of dATP with luciferase. dATP $\alpha$ S is efficiently incorporated by the polymerase, generating pyrophosphate, but does not interact with luciferase [20]. After completion of the reaction, the content of each well was serially diluted for comparison of extension analysis (PPi concentration). Extension and real-time luminometric monitoring was performed at room temperature either in an IVIS™ imaging system (Xenogen, Alameda, CA USA), or in an Lmax™ microplate luminometer (Molecular Devices, Sunnyvale, CA, USA). A luminometric reaction mixture was added to the substrate at different concentrations (extended primed single-stranded DNA or self-primed oligonucleotide). The 40  $\mu$ l bioluminescence assay mixture contained: 3.0  $\mu$ g luciferase (Promega, USA), 50 mU recombinant ATP-sulfurylase (Sigma, USA), 0.1 M Tris-acetate (pH 7.75), 0.5 mM EDTA (Sigma, USA), 5 mM Mg-acetate (Sigma, USA), 0.1% (w/v) bovine serum albumin (Sigma, USA), 2.5 mM dithiothreitol (Sigma, USA), 10  $\mu$ M adenosine 5'-phosphosulfate (APS) (BIOLOG Life Science Institute, Bremen, Germany), 0.4 mg polyvinylpyrrolidone/ml (molecular weight 360000) and 100  $\mu$ g D-luciferin/ml (BioThema, Dalara, Sweden), and the emitted light was detected in real time and measured after approximately 45 s with 1 s and 10 s integration times for the CCD imaging system and luminometer, respectively.

##### 3.1.4. ATP assay

Using the fully automated plate-based PSQ96™ pyrosequencing instrument (Pyrosequencing AB, Uppsala, Sweden), ATP was dispensed (1 pmol or 5 pmol) into a 40  $\mu$ l mixture containing 3.0  $\mu$ g luciferase (Promega, USA), 0.1 M Tris-acetate (pH 7.75), 0.5 mM EDTA (Sigma, USA), 0.1% bovine serum albumin (Sigma), 2.5 mM dithiothreitol (Sigma), 0.4 mg polvinylpyrrolidinone/ml (MW 360,000), and 100  $\mu$ g D-luciferin (BioThema, Dalara, Sweden), and the emitted light was detected in real time.

##### 3.1.5. Detection devices

To estimate the quantity of the target nucleic acid, we counted the photons generated by the BRC process. The general luciferase generation of photons has a quantum efficiency (Q.E.) of approximately 0.88 per consumed ATP molecule, and the maximum wavelength, depending on the type of luciferase, is in the visible range of the optical spectrum (e.g., 565 nm for firefly luciferase) [26,27].

Various photosensitive devices developed to detect bioluminescent signals have been used to detect light from the regenerative phenomenon. These devices include photomultiplier tubes (PMTs), charge-coupled devices (CCDs),



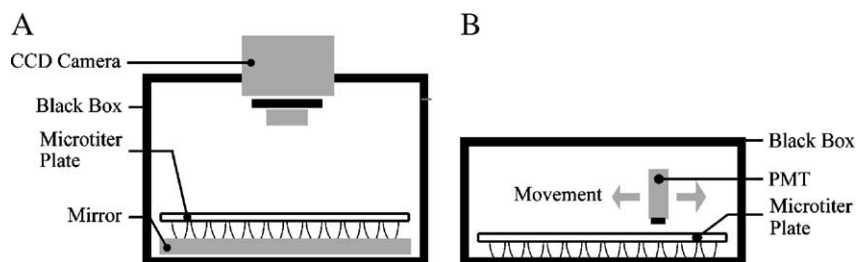


Fig. 4. (A) CCD camera system that simultaneously measures the light from the reference buffer and target sample, and (B) PMT imaging system in a luminometer.

and photodiodes. The photosensitive device can be in close proximity to the BRC reaction to receive the incident photons directly, or at a distance from the reaction buffer with a light-coupling device (e.g., optical fiber or mirror system) to convey photons from the sample to the detector.

In our experiments we used both a cooled CCD camera imaging system (IVIS; Xenogen, Alameda, CA USA) and a luminometer (Lmax™; Molecular Devices, Sunnyvale, CA, USA) that employed a single PMT detector. The light-coupling efficiencies of each system (including path loss), from the microtiter plate where the DNA samples were located to the sensor, were approximately 0.012% and 8% for the CCD and PMT systems, respectively, as shown in Fig. 4.

In the CCD imaging system a 96-well microtiter plate with multiple DNA samples was placed 18 cm below the lens of the camera (Fig. 4A), and a 384-well microtiter plate was inserted in the instrument chamber of the luminometer,

where a PMT directly moves into close proximity (1 cm) of the sample for reading (Fig. 4B).

### 3.2. Experimental results and discussion

#### 3.2.1. Kinetics of the BRC system

To observe the kinetics of the BRC system and compare it to other ATP-based assays, we introduced different ATP concentrations into the enzymatic complex and measured the light intensity for multiple experiments. Our first observation was that the total photon generation was orders of magnitude higher than would be expected from the number of ATP molecules present in the solution (Figs. 5 and 6). If luciferase were the only enzyme controlling the photon-generating kinetics, then we would expect, in the best case, a single photon per ATP molecule. We can conclude, then, that a regenerative process is present in our enzymatic system. By measuring the light intensity over a

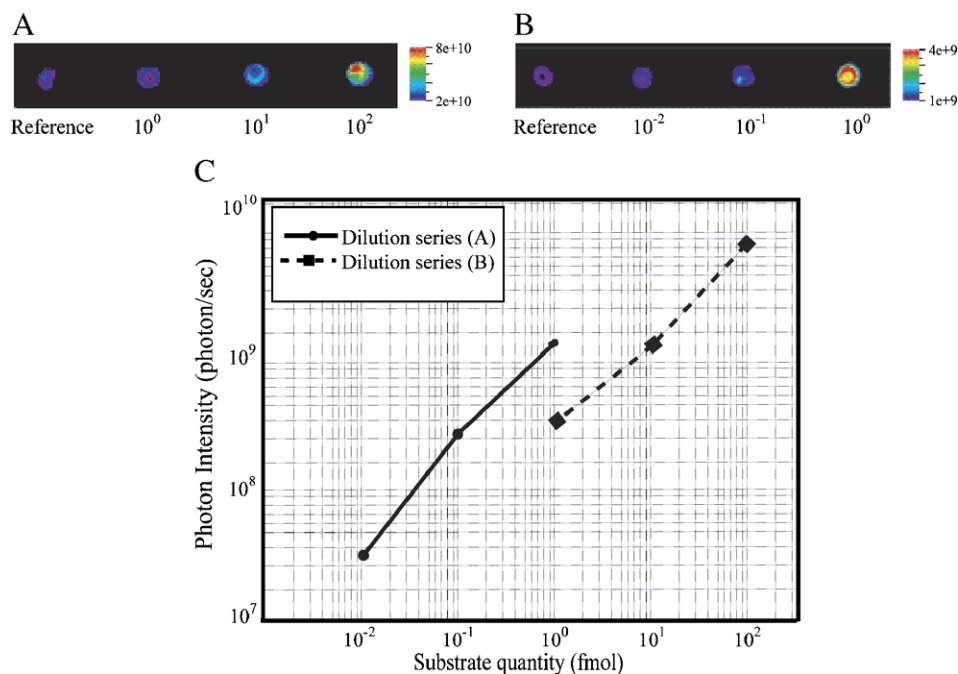


Fig. 5. Photon intensity (photon/s) measured by CCD imaging systems in a 96-well microtiter plate format from (A) 1–100 fmol 40 bp oligo-loop and (B) 10 amol to 1 fmol 230 bp PCR product. A normalized-value plot of intensities from ranges (A) and (B) is shown in (C). Note that camera threshold values differed for these images, so that the visual intensity in (A) and (B) is not representative of the calculated and normalized values shown in (C). Camera threshold for (A)= $2e+10$ . Camera threshold for (B)= $1e+9$ .

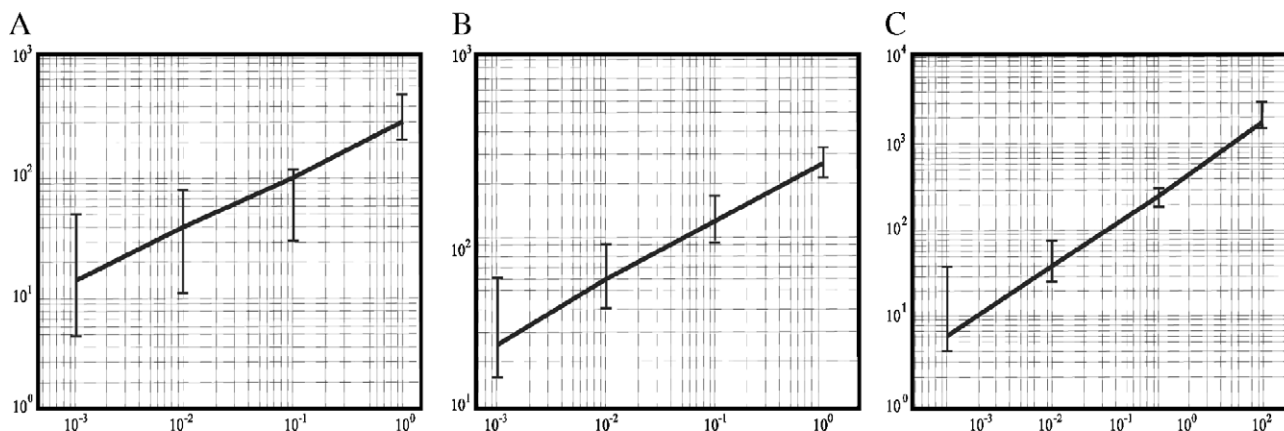


Fig. 6. Relative luminescence units from incorporation of dNTPs, measured by a luminometer, for 1 fmol to 1 amol of (A) ATP, (B) 40 bp oligonucleotide loop, (C) 230 bp PCR product. Results for each dilution are independent but normalized.

long interval we observed that, although the light intensity was almost constant, using 1 and 5 pmol ATP in 40  $\mu$ l reaction, a slow exponential decay with a time constant of approximately 10 min did exist (Fig. 3). This observation also fits well with our hypothesis, that the energy source for photon emission comes from APS and luciferin, which eventually would be consumed and ultimately become the limiting factors for the luciferase and ATP-sulfurylase kinetics (Fig. 3E and F).

### 3.2.2. Background noise correction

By measuring the light intensity from different samples, we observed a background signal even without the addition of excess PPI from DNA polymerization. The level of this background, which we used as a reference for all our measurements, was comparable up to 0.1 fmol of ATP in 40  $\mu$ l (Fig. 5). This background varied up to almost 2.5-fold between independent reaction mixes, but remained constant within a given experiment. There are two possible explanations for the background signal. First, there may be PPI or ATP residue from either luciferase, reaction buffer, or ATP-sulfurylase mixes, or there may be intrinsic bioluminescence of luciferase at high enzyme concentrations. In our experiments the background light was obtained by running a sample-free reaction as a reference, and the signal derived from this reference was subtracted from the signal of test samples. By employing this approach we were able to successfully differentiate between nucleic acid concentrations ranging over five orders of magnitude, from 1 amol ( $10^{-18}$  mol) to 0.1 pmol ( $10^{-12}$  mol) (PCR product and self-primed oligo; Figs. 5 and 6).

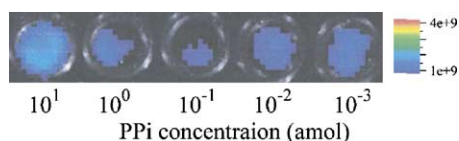


Fig. 7. Measurement of background noise by addition of different concentrations of PPI to the reaction mixture.

Notably, the BRC system shows lower background noise from APS (adenosine phosphosulfate), which is known to be a weak substrate for firefly luciferase [17]. This can be attributed to the small amount of ATP and PPI present in the system at steady state and results in much higher sensitivity than might otherwise be expected. As shown in Fig. 7, addition of 0.1 amol of PPI prior to the reaction reduces the background noise to almost zero which increases both the dynamic range and sensitivity of the reaction.

### 3.2.3. Signal and sensitivity

Using the CCD camera for measurements we were able to detect a signal from 10 amol to 100 fmol of the target molecule using both the self-primed oligonucleotide and a 230 bp PCR product (Fig. 5). In the BRC system, the background luminescent light was approximated to be 80 amol of equivalent ATP molecules in 40  $\mu$ l reaction buffer, which corresponds to a concentration of 2.5 pM of substrate for luciferase. The integration time was 1 s.

By contrast, sensitivity was decreased and noise increased when using the luminometer. By increasing the integration time from 1 s to 10 s, however, we found the performance of the two detectors to be comparable. We were able to detect 1 amol to 100 amol of target in 20  $\mu$ l for both the self-primed oligonucleotide (oligo-loop) and the 230 bp PCR product (MBP) with the luminometer (Fig. 6).

## 4. Summary

In BRC system the bioluminescence photon emission rate was steady and was a monotonic function of the introduced PPI. The regeneration characteristic of the BRC system stabilized the light intensity and made the photon emission rate relatively steady for long periods of time. This system could potentially generate orders of magnitude more photons than most luciferase assays. The steady photon emission in this system is also a linear function of the nucleic acid concentration for less than 10 nM and, by adjusting the

integration time, we are able to achieve a dynamic range of five orders of magnitude for the nucleic acid quantity using commercially available CCD imaging systems and luminometers. This methodology can be used as an alternative label-free pyrophosphate optical detection, such as for ATP and pyrophosphate present in target cells and/or microorganisms in samples, or for those catalyzed by DNA ligase or adenylate cyclase, as well as for parallel in vitro nucleic acid quantification for detecting DNA at concentrations of 1 amol. Direct applications of BRC include gene expression, pathogen profiling, DNA or RNA quantification and single nucleotide polymorphism (SNP) detection. The practical challenges of this approach include the reduction of background light, purification of enzyme and substrate, and biochemical optimization for each application.

### Acknowledgments

The authors wish to thank the Molecular Biophotonics Laboratory (Stanford University) for the use of their IVISTM imaging. We are grateful to Robert G. Eason for his valuable comments on this manuscript, and to Abbas El-Gamal and Khaled Salama for insightful discussions. This study was supported, in part, by a grant from the National Institutes of Health, HG 000205, CA88303 (CHC), and unrestricted gifts from the Bio-X Program at Stanford.

### References

- [1] C.A. Heid, J. Stevens, K.J. Livak, P.M. Williams, Real time quantitative PCR, *Genome Res.* 6 (1996) 986–994.
- [2] U.E. Gibson, C.A. Heid, P.M. Williams, A novel method for real time quantitative RT-PCR, *Genome Res.* 6 (1996) 995–1001.
- [3] S. Tyagi, D.P. Bratu, F.R. Kramer, Multicolor molecular beacons for allele discrimination, *Nat. Biotechnol.* 16 (1998) 49–53.
- [4] S. Tyagi, F.R. Kramer, Molecular beacons: probes that fluoresce upon hybridization, *Nat. Biotechnol.* 14 (1996) 303–308.
- [5] M. Schena, D. Shalon, R.W. Davis, P.O. Brown, Quantitative monitoring of gene expression patterns with a complementary DNA microarray, *Science* 270 (1995) 467–470.
- [6] D. Shalon, S.J. Smith, P.O. Brown, A DNA microarray system for analyzing complex DNA samples using two-color fluorescent probe hybridization, *Genome Res.* 6 (1996) 639–645.
- [7] A.C. Pease, D. Solas, E.J. Sullivan, M.T. Cronin, C.P. Holmes, S.P. Fodor, Light-generated oligonucleotide arrays for rapid DNA sequence analysis, *Proc. Natl. Acad. Sci. U. S. A.* 91 (1994) 5022–5026.
- [8] E.M. Southern, Detection of specific sequences among DNA fragments separated by gel electrophoresis, *J. Mol. Biol.* 98 (1975) 503–517.
- [9] M. Schena, D. Shalon, R. Heller, A. Chai, P.O. Brown, R.W. Davis, Parallel human genome analysis: microarray-based expression monitoring of 1000 genes, *Proc. Natl. Acad. Sci. U. S. A.* 93 (1996) 10614–10619.
- [10] V. Jansson, K. Jansson, Enzymatic chemiluminescence assay for inorganic pyrophosphate, *Anal. Biochem.* 304 (2002) 135–137.
- [11] V. Derbyshire, P.S. Freemont, M.R. Sanderson, L. Beese, J.M. Friedman, C.M. Joyce, et al., Genetic and crystallographic studies of the 3',5'-exonucleolytic site of DNA polymerase I, *Science* 240 (1988) 199–201.
- [12] F. Renosto, R.L. Martin, I.H. Segel, ATP sulfurylase from *Penicillium chrysogenum*. Molecular basis of the sigmoidal velocity curves induced by sulfhydryl group modification, *J. Biol. Chem.* 262 (1987) 16279–16288.
- [13] I.J. MacRae, I.H. Segel, A.J. Fisher, Crystal structure of ATP sulfurylase from *Penicillium chrysogenum*: insights into the allosteric regulation of sulfate assimilation, *Biochemistry* 40 (2001) 6795–6804.
- [14] T.O. Baldwin, V.A. Green, Purification of firefly luciferase from recombinant sources, *Methods Enzymol.* 305 (2000) 180–188.
- [15] W.D. McElroy, M.A. DeLuca, Firefly and bacterial luminescence: basic science and applications, *J. Appl. Biochem.* 5 (1983) 197–209.
- [16] P. Nyren, Enzymatic method for continuous monitoring of DNA polymerase activity, *Anal. Biochem.* 167 (1987) 235–238.
- [17] P. Nyren, A. Lundin, Enzymatic method for continuous monitoring of inorganic pyrophosphate synthesis, *Anal. Biochem.* 151 (1985) 504–509.
- [18] T. Tabary, L.Y. Ju, J.H. Cohen, Homogeneous phase pyrophosphate (PPi) measurement (H3PIM). A non-radioactive, quantitative detection system for nucleic acid specific hybridization methodologies including gene amplification, *J. Immunol. Methods* 156 (1992) 55–60.
- [19] P. Nyren, S. Karamohamed, M. Ronaghi, Detection of single-base changes using a bioluminometric primer extension assay, *Anal. Biochem.* 244 (1997) 367–373.
- [20] M. Ronaghi, S. Karamohamed, B. Pettersson, M. Uhlen, P. Nyren, Real-time DNA sequencing using detection of pyrophosphate release, *Anal. Biochem.* 242 (1996) 84–89.
- [21] M. Ronaghi, M. Uhlen, P. Nyren, A sequencing method based on real-time pyrophosphate, *Science* 281 (1998) 363–365.
- [22] M.E. Dahlberg, S.J. Benkovic, Kinetic mechanism of DNA polymerase I (Klenow fragment): identification of a second conformational change and evaluation of the internal equilibrium constant, *Biochemistry* 30 (1991) 4835–4843.
- [23] L. Brovko, O. Gandel'man, T. Polenova, N. Ugarova, Kinetics of Bioluminescence in the Firefly Luciferin-Luciferase System, *Biochem. (Moscow)* 59 (1994) 195–201.
- [24] F.G.R. Gimblett, Introduction to the Kinetics of Chemical Chain Reactions, Mc Graw-Hill, New York, 1970; T.E. Harris, Theory of Branching Processes, Dover Phoenix Edition, New York, 1996.
- [25] M.O. Vlad, F. Moran, Y. Rodriguez, J. Ross, Delayed response in tracer experiments and fragment-carrier approach to transit time distributions in nonlinear chemical kinetics, *Int. J. Bifurc. Chaos* 12 (2002) 2599–2618.
- [26] N. Kajiyama, T. Masuda, H. Tatsumi, E. Nakano, Purification and characterization of luciferases from fireflies, *Luciola cruciata* and *Luciola lateralis*, *Biochim. Biophys. Acta* 1120 (1992) 228–232.
- [27] N. Kajiyama, E. Nakano, Isolation and characterization of mutants of firefly luciferase which produce different colors of light, *Protein Eng.* 4 (1991) 691–693.